Proceedings of the 11th World Congress on Mechanical, Chemical, and Material Engineering (MCM'25)

Paris, France - August, 2025 Paper No. HTFF 111 DOI: 10.11159/htff25.111

Cross-Stream Measurements in a Small Aspect-Ratio Rectangular Jet

Mohammad Azad

St. Francis Xavier university
4130 University Avenue, Antigonish, Canada
mazad@stfx.ca

Abstract - The results of an experimental investigation of an isothermal, incompressible, and unforced rectangular jet of air issuing into still air surroundings are presented. The sharp-edged rectangular orifice had an aspect ratio of 2. The results obtained in a sharp-edged round jet, with the same exit area as that of the rectangular one, are included for comparison. The Reynolds number, based on the equivalent diameter of the rectangular orifice, was 1.61×10^5 . A DANTEC P51 x-array hot-wire probe, and a pitot-static tube were used to make measurements. The shape of the mean streamwise velocity contour maps of the rectangular jet changes throughout the downstream distance investigated. The mean streamwise vorticity contour map close to the exit plane shows four counter-rotating pairs of vortices aligned with the four corners of the rectangular orifice. The sense of rotation of the vortex pairs indicates inflow of the ambient fluid into the jet through the orifice corners. Indeed, the secondary flow velocity vectors at the same location show inflow of the ambient fluid through the corners. The mean static pressure contour map at the same location shows four negative pressure cells aligned with the corners of the rectangular orifice, implying inflow of the ambient fluid through these corners. The four counter-rotating vortex pairs initially aligned with the corners merge into a single vortex at seven equivalent diameters downstream of the exit plane.

Keywords: Turbulence, Jet, Mixing, Turbulent Jet, Rectangular, Orifice

1. Introduction

Rectangular turbulent free jets have been studied extensively over the past few decades [1-5]. Many of the researchers have reported that the mean streamwise centreline velocity decay profile of a rectangular jet consists of three regions: the potential core region, the characteristic decay region, and the axisymmetric decay region [1, 3, 4]. Quinn [5] did experiments in four jets issuing from rectangular orifices with aspect ratios of 2, 5, 10, and 20 and found that mixing in the near field increased with the aspect ratio of the rectangular orifice, as long as the flow was three dimensional. However, the difference in the far-field mixing rates, as deduced from the mean streamwise centreline velocity decay and the spreading rates, of the rectangular jets with aspect ratios of 2 and 5 was insignificant. The mean streamwise centreline velocity decay rate increased significantly in the rectangular jets with aspect ratios of at least 10. Quinn [6] reported the results of detailed measurements in a rectangular jet issuing from an orifice with an aspect ratio of 20. The mean streamwise vorticity contour maps showed that mixing in the near field of this jet was dominated by counter-rotating pairs of vortices. Also, the jet spread monotonically in the central plane containing the short sides and contracted initially on the central plane containing the long sides. Zaman [7] conducted an experimental study on rectangular jets with aspect ratios of 1, 2, 4, 8, 16, and 32. His results showed no distinct difference among the rectangular jets with aspect ratios of 1, 2, 4, and 8. Moreover, these jets did not have an increased mixing over the round jet considered in the study. However, the rectangular jets with aspect ratios of 16 and 32 had significantly higher mixing rates than the smaller aspect ratio rectangular jets and the round jet. Some authors have reported that square (rectangular with an aspect ratio of 1) and rectangular jets with small aspect ratios had higher mixing rates than a round jet [8, 9]. This finding contradicts the results of Quinn [5] and Zaman [7], who attributed the disagreement to the difference in the initial conditions. The quantities measured in previous studies were limited to the jet centreline and planes containing the major or minor axis. In some cases, the mean streamwise velocity and turbulence intensity contour maps on the planes perpendicular to the flow direction were reported. It appears that no detailed measurements, especially those in cross-planes have thus far been made in a rectangular jet issuing from a small aspect ratio orifice, except some crossstream mean streamwise velocity contour maps. In this paper, mean streamwise velocity contour maps, mean streamwise vorticity and mean static pressure contours on the cross-sectional planes and secondary flow velocity vectors will be presented.

2. Experimental set-up and equipment

A detailed description of the flow facility and equipment has been given elsewhere [10]. Very briefly, a blow down flow facility, consisting of a centrifugal fan, a diffuser, a settling chamber, and a contraction, was used. The centrifugal fan, supported on anti-vibration neoprene pads, drew air and delivered it via a flexible duct to the orifices through the diffuser, settling chamber and the contraction. The diffuser, which had a divergence angle of 9°, was fitted with a honeycomb and a mesh-wire screen. The settling chamber contained seven mesh-wire screens of 69% porosity. The upstream end of the contraction was circular and the downstream end, which was capped by the orifices, was square. The contraction ratio was 283.

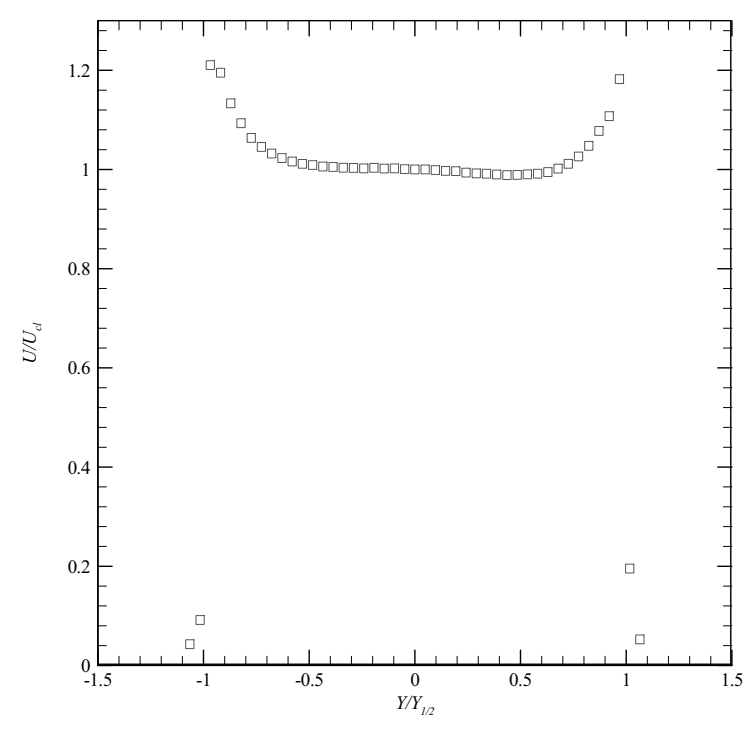


Fig. 1: Mean streamwise velocity profile at $X/D_e = 0.035$.

A three-dimensional traversing system, also supported on anti-vibration neoprene pads, was used to move the measuring probes in the flow field. The positioning accuracy was 0.3 mm in the streamwise direction and 0.01 mm in the spanwise and lateral directions.

A pitot-static tube with an ellipsoidal head and four circumferentially located static pressure holes and a DANTEC P51 x-array hot-wire probe were used to make the measurements. The hot-wire probe was calibrated for velocity and yaw in situ online according to Bradshaw [11]. The velocity calibration was done against the known values obtained by the pitot - static tube in the velocity range of 8 m/s to 65 m/s. The yaw calibration was performed against the hot-wire voltages obtained in an angular range of -35° to 35° in steps of 5°. The temperature was monitored by a thermocouple placed close to the hot-wire probe and the pitot-static tube and corrections for temperature drift were made in the data reduction software following Bearman [12]. The signals from the hot-wire probe and the thermocouple were linearized and digitized as described in Quinn [10].

3. Initial conditions

The mean streamwise velocity profile (U/U_{cl}) vs. $Y/Y_{1/2}$ of the rectangular jet at $X/D_e = 0.035$ is shown in Fig. 1, where, U is the treamwise component of the mean velocity vector, U_{cl} is the value of U on the jet centerline, Y is

the spanwise coordinate, $Y_{1/2}$ is the jet half-velocity width in the Y-direction, X is the streamwise coordinate, and D_e is the equivalent diameter of the rectangular orifice. The U/U_{cl} profile is fairly uniform in the central region with pronounced off-center peaks close to the edges of the jet. The off-center peaks in the mean streamwise velocity profiles are typical not only of rectangular jets but also of other orifice jets [5, 10, 13, 14].

The corresponding Y-profiles of the streamwise $(\sqrt{u^2} / U_{cl})$ and spanwise $(\sqrt{v^2} / U_{cl})$ turbulence intensities, also at $X/D_e=0.035$, are shown in Figs. 2(a) and 2(b), respectively. Here, $\sqrt{u^2}$ and $\sqrt{v^2}$ are root-mean-squares of the fluctuating streamwise and spanwise velocities, respectively. The $\sqrt{u^2} / U_{cl}$ profile is flat in the central region where the U profile is nearly uniform. The value of $\sqrt{u^2} / U_{cl}$ is 0.4% at the centre and reaches a maximum value (around 8%) in the shear layers. The $\sqrt{v^2} / U_{cl}$ profile is similar to the $\sqrt{u^2} / U_{cl}$ profile but with lower values, as expected. The value of $\sqrt{v^2} / U_{cl}$ is about 0.1% in the central region and it increases to 2% in the shear layers.

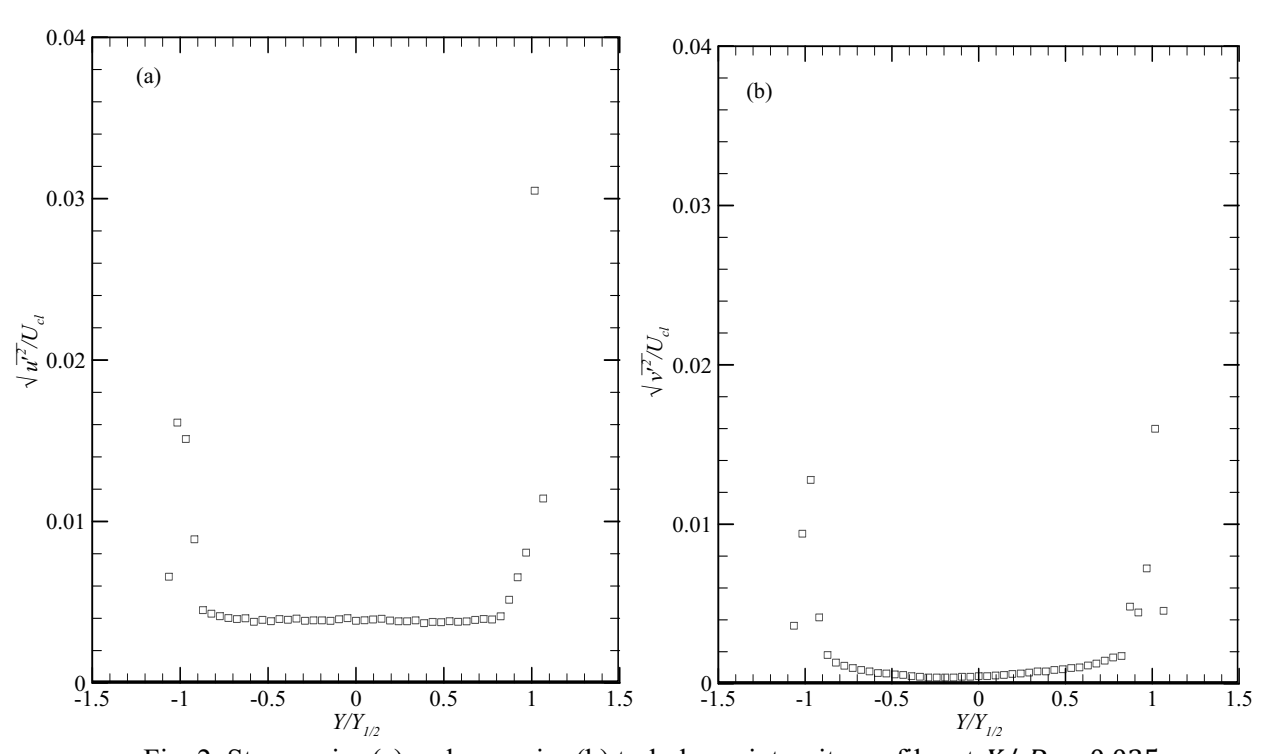


Fig. 2: Streamwise (a) and spanwise (b) turbulence intensity profiles at $X/D_e = 0.035$.

The uncertainties in different quantities were calculated using the multiple-sample theorem method in Tavoularis [15], with 95% confidence interval. The data from the measurements at $(X/D_{e'}Y/D_{e'})=(6.17,\ 0.28)$, where the turbulence intensities had the highest values, were used. The uncertainties in $U,\ \bar{u}^2,\ \bar{v}^2,\ P_s$ (mean static pressure) and Ω_X (mean streamwise vorticity) are $\pm 1.34\%, \pm 3.62\%, \pm 4.54\%, \pm 0.56\%$, and $\pm 20.48\%$, respectively.

4. Results and discussion

4.1. Normalized mean streamwise velocity contour maps

The normalized mean streamwise velocity (U/U_{cl}) contour maps for the rectangular jet at several locations downstream are shown in Fig. 3. At $X/D_e = 0.14$, the shapes of the U/U_{cl} contours resemble that of the orifice and the contour levels

are very closely spaced with a large high-velocity area; these observations indicate that a very little mixing has taken place in the jet. At $X/D_e=0.25$, the shape of the contours is similar to that of the orifice except that the corners of the rectangle are more rounded. As will be shown later in the secondary flow velocity vectors and the mean streamwise vorticity contour maps, the inflow of the ambient fluid into the jet occurs through the corners and outflow of the jet fluid to the ambient occurs through the sides of the rectangular jet, which causes the corners move toward the centroid of area of the rectangle and the sides to move outward from the centroid. This phenomenon causes the corners to be rounded and the jet to become rhomboidal at $X/D_e=3.0$. A rhomboidal shape has also been observed in a rectangular jet with an aspect ratio of 1.5 approximately at $X/D_e=2.9$ by Tsuchiya *et al* [16]. The U/U_{cl} contours are very widely spaced at $X/D_e=7.0$ and the contour maps are much larger compared to the locations upstream. It is noteworthy that the initial orientation of the axes has changed at this location, namely, the short side is aligned with the Y- direction and the long side is aligned with the Z- direction (lateral coordinate). This is usually referred to as axis-switching. This change in orientation of the axes was indicated by the cross-over in half-velocity widths at $X/D_e=2$ (not shown here). Throughout the downstream distance investigated, the contour levels become wider spaced, indicating increased mixing in the jet. However, the axis of symmetry at $X/D_e=10$ and 15 appears to be rotated by 45 ° compared to the locations upstream. The present jet loses its initial rectangular shape at $X/D_e=3$ and becomes elliptic at $X/D_e=7$.

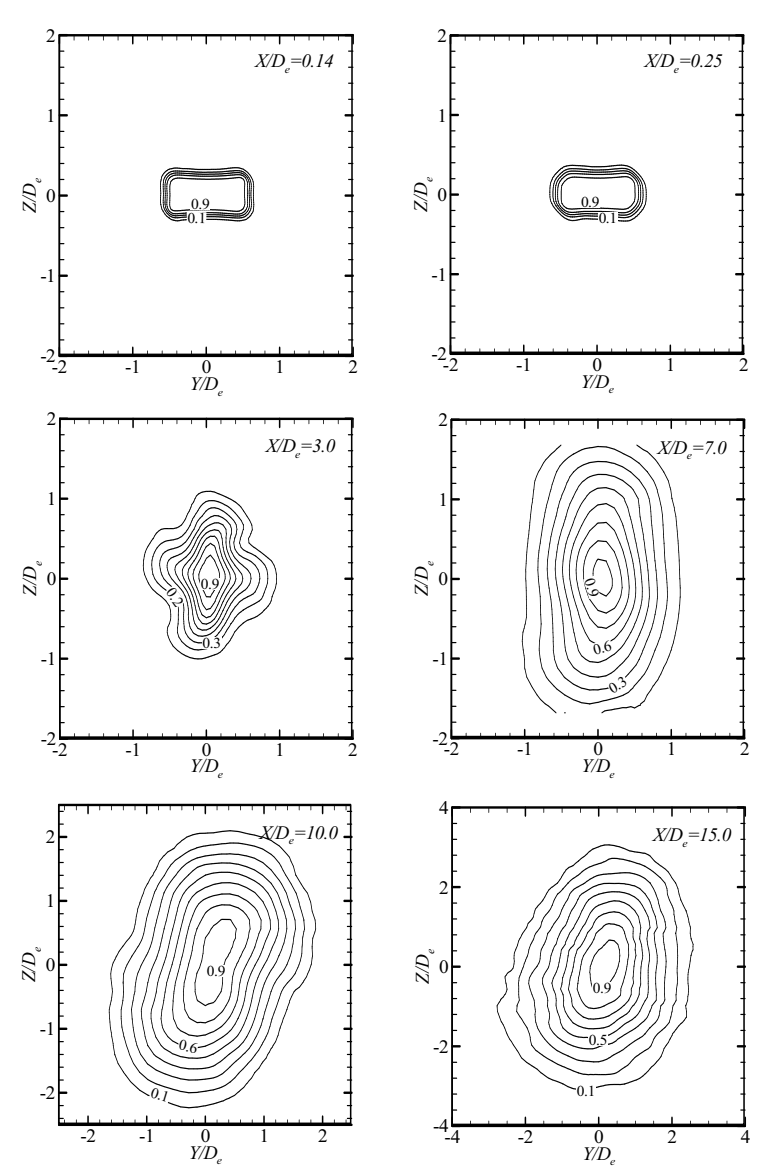


Fig. 3: Mean streamwise velocity contour maps.

4.2. Mean static pressure contour maps

The mean static pressure contour maps $(2(P_s - P_{atm})/\rho U_{cl}^2)$ for the rectangular jet at $X/D_e = 0.14$, $X/D_e = 3.0$ and at $X/D_e = 7.0$ are shown in Fig. 4, where P_{atm} is the atmospheric pressure and ρ is the density of air. The continuous-lines in the figure represent positive pressures and the dashed-lines represent negative pressures. At $X/D_e = 0.14$, the pressure in the central region of the jet is positive, consistent with the mean static pressure distribution on the jet centreline (not shown here), and negative in the corner regions of the rectangular jet. Flow will, therefore, be induced from the corners into the central region of the jet, as was indicated by the normalized mean streamwise velocity contour maps and will shortly be seen in the mean streamwise vorticity contour map and secondary flow velocity vectors at $X/D_e = 0.14$. Also, the higher than ambient pressure in the central region of the jet will push the jet fluid to the ambient through the sides of the rectangle. At $X/D_e = 3.0$ and $X/D_e = 7.0$, the pressure is negative anywhere in the jet, which will bring more ambient fluid into the jet and the pressure will keep increasing towards the atmospheric value.

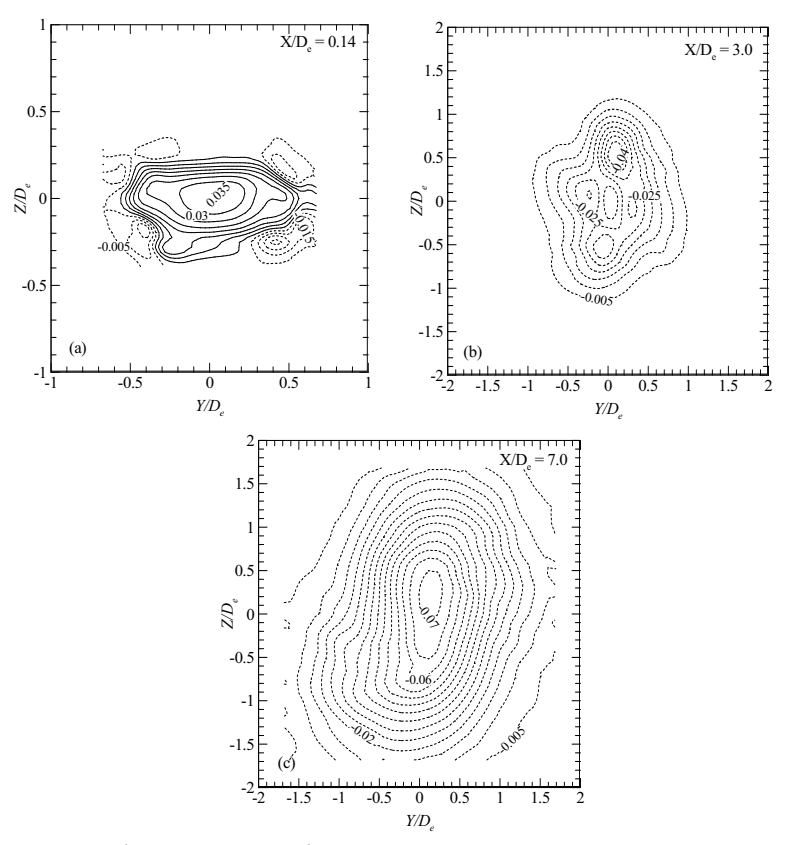


Fig. 4: Mean static pressure contour maps.

4.3. Secondary flow velocity vector

The secondary flow velocity vectors for the rectangular jet at the same locations where the mean static pressure contour maps have been presented are shown in Fig. 5. The secondary flow velocity vectors at $X/D_e = 0.14$ show that the ambient fluid flows into the jet through the corners, as was indicated by the mean static pressure contour maps. At $X/D_e = 3.0$, two clockwise rotating cells aligned approximately with one of the diagonals of the rectangular jet are clearly present. Further downstream, at $X/D_e = 7.0$, these two clockwise rotating cells merge into a single cell covering the whole jet.

4.4. Normalized mean streamwise vorticity contour maps

The normalized mean streamwise vorticity ($\Omega_X D_e / U_{cl}$) contour maps at the same locations where the mean static pressure contour maps and the secondary flow velocity vectors have been shown are presented in Fig. 6. In this figure, the continuous-lines represent positive and counterclockwise rotating vortices, and the dashed-lines represent negative and clockwise rotating vortices. At $X/D_e = 0.14$, four pairs of clockwise and counterclockwise rotating vortices aligned with the four corners of the rectangular jet are present. Orientations of the vortex pairs are such that flow of the ambient fluid into the jet occurs through the corners and outflow of the jet fluid to the ambient occurs through the sides of the jet, consistent with the other results discussed in previous two sections. Four pairs of the rotating cells are still present at $X/D_e = 3.0$, although they appear to be tilted. These cells merge into a single vortex at $X/D_e = 7.0$ and still appear to be tilted by 45°.

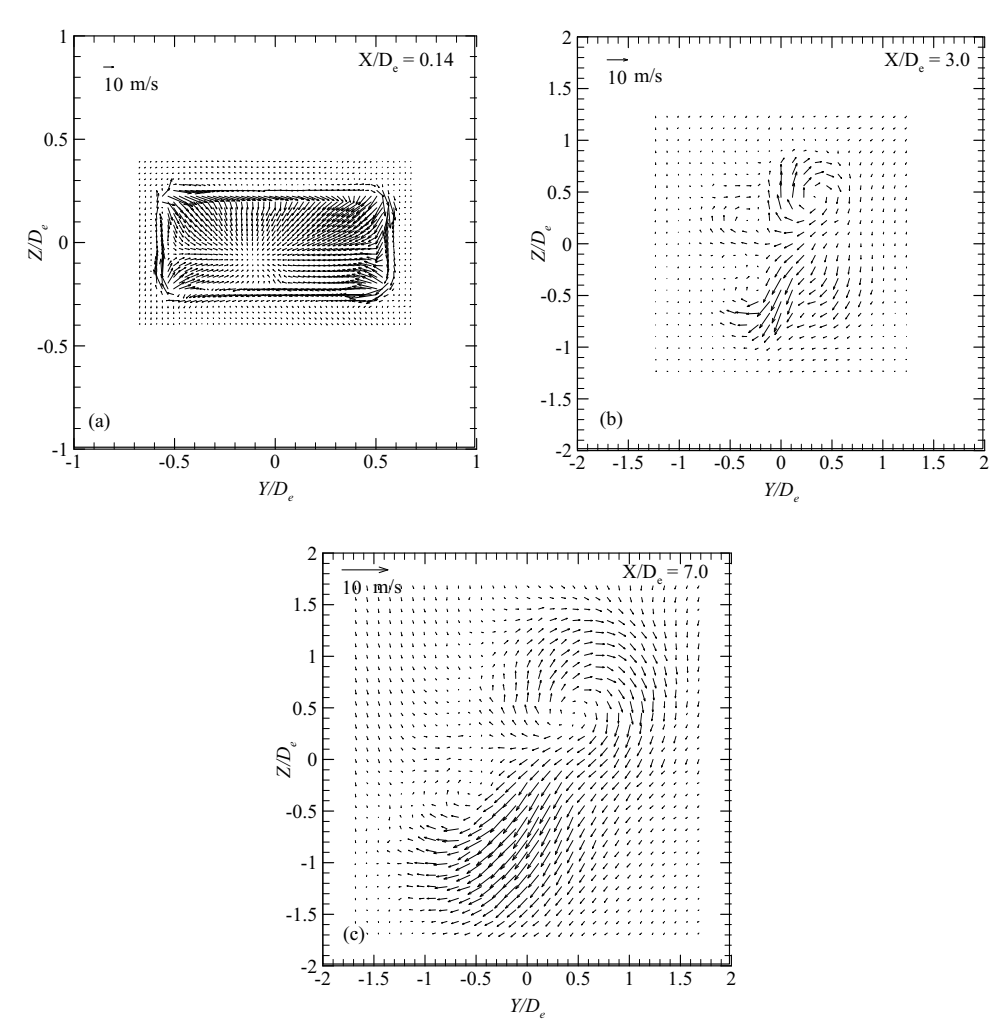


Fig. 5: Secondary flow velocity vectors.

5. Conclusion

An isothermal, incompressible, and unforced rectangular jet issuing from a sharp-edged orifice with an aspect ratio of 2 was investigated experimentally. The Reynolds number, based on the equivalent diameter of the rectangular orifice (same as the diameter of the round orifice), was 1.61×10^5 . A pitot-static tube was used to measure mean streamwise velocities at several locations downstream of the jet exit plane; the mean streamwise velocity contour maps, spreading and entrainment results were obtained from those measurements. The pitot-static tube was also used to measure mean static pressure on the jet centreline and in planes perpendicular to the flow. A DANTEC P51 x-array hot-wire probe was used to measure three components of the mean velocity vector. From these measurements, secondary flow velocity vectors, and mean streamwise vorticity contour maps were obtained. Some results obtained from experiments in a sharp-edged round jet are also presented. The mean streamwise vorticity contour maps of the rectangular jet show that four pairs of counter-rotating vortices generate at the four corners of the rectangular orifice, which draw air from the ambient into the jet through the corners and push the jet fluid out to the ambient through the sides. This finding is complemented by the mean static pressure contour maps and the secondary flow velocity vectors.

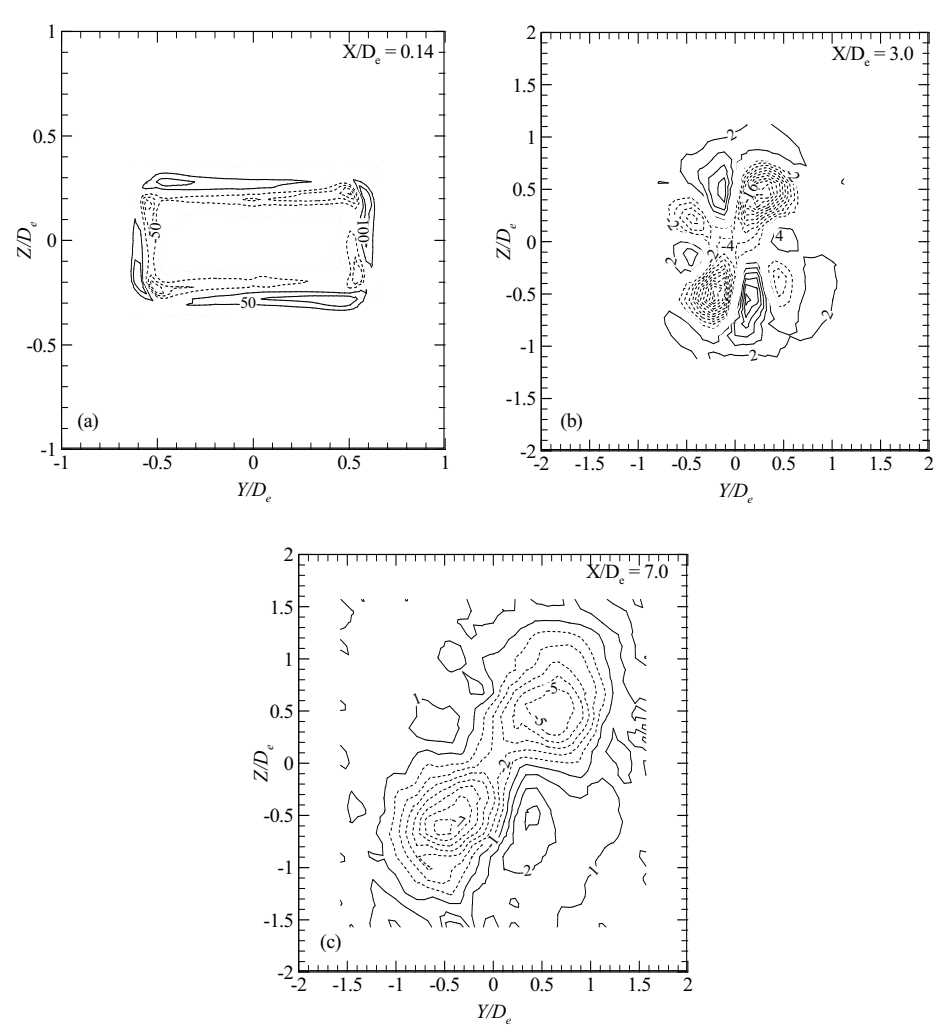


Fig. 6: Mean streamwise vorticity contour maps.

References

- [1] P. M. Sforza, M. H. Steiger, and N. Trentacoste, "Study on three-dimensional viscous jets," *AIAA Journal*, vol. 4, no. 5, pp. 800-806, 1966.
- [2] A. A. Sfeir, "The velocity and temperature fields of rectangular jets," *Int. J. Heat Mass Transfer*, vol. 19, no. 3, pp. 1289-1297, 1976.
- [3] A. Krothapalli, D. Baganoff, and K. Karamcheti, "On the mixing of a rectangular jet," *J. Fluid Mech.*, vol. 107, pp. 201-220, Jun. 1981.
- [4] A. A. Sfeir, "Investigation of three-dimensional turbulent rectangular jets," *AIAA Journal*, vol. 17, no. 10, pp. 1055-1060, 1979.
- [5] W. R. Quinn, "Turbulent free jet flows issuing from sharp-edged rectangular slots: The influence of slot aspect ratio," *Exp. Therm. Fluid Sci.*, vol. 5, no. 2, pp. 203-215, 1992.
- [6] W. R. Quinn, "Development of a large-aspect-ratio rectangular turbulent free jet," *AIAA Journal*, vol. 32, no. 3, pp. 547-554, 1994.
- [7] K. B. M. Q. Zaman, "Spreading characteristics of compressible jets from nozzles of various geometries," *J. Fluid Mech.*, vol. 383, pp. 197-228, Mar. 1999.

- [8] J. Mi, G. J. Nathan, and R. E. Luxton, "Centreline mixing characteristics of jets from nine differently shaped nozzles," *Experiments in Fluids*, vol. 28, no. 1, pp. 93-94, 2000.
- [9] J. Mi and G. J. Nathan, "Statistical properties of turbulent free jets issuing from nine differently-shaped nozzles," *Flow, Turbulence and Combustion*, vol. 84, no. 4, pp. 583-606, 2010.
- [10] W. R. Quinn, "Upstream nozzle shaping effects on near-field flow in round turbulent free jets," *Eur. J. Mech. B/Fluids*, vol. 25, no. 3, pp. 279-301, 2006.
- [11] P. Bradshaw, An Introduction to Turbulence and its Measurement, Pergamon Press, Oxford, 1975, chap. 5.
- [12] P. W. Bearman, "Corrections for the effect of ambient temperature drift on hot-wire measurements in incompressible flow," *DISA Info*, vol. 11, no. 11, pp. 25-30, 1971.
- [13] J. Mi, G. J. Nathan, and D. S. Nobes, "Mixing characteristics of axisymmetric free jets from a contoured nozzle, an orifice plate and a pipe," *J. Fluids Eng.*, vol. 123, no. 4, pp. 878-883, 2001.
- [14] W. R. Quinn and J. Militzer, "Experimental and numerical study of a turbulent free square jet," *Physics of Fluids*, vol. 31, no. 5, pp. 1017-1025, 1988.
- [15] S. Tavoularis, Measurement in Fluid Mechanics, Cambridge University Press, Cambridge, 2005, chap. 3.
- [16] Y. Tsuchiya, C. Horikoshi, and T. Sato, "On the spread of rectangular jets," *Experiments in Fluids*, vol. 4, no. 4, pp. 197-204, 1986.